

# A comparative study of granular solid-like and fluid-like constitutive laws

Retief Lubbe<sup>1,\*</sup>, Hongyang Cheng<sup>1</sup>, Stefan Luding<sup>1</sup>, and Vanessa Magnanimo<sup>1</sup>

<sup>1</sup>Engineering Technology, University of Twente, 7522 NB Enschede, Netherlands

**Abstract.** Continuum models are efficient tools for simulating granular materials at the macroscopic scale. These models rely on constitutive laws that typically capture only solid-like behavior or fluid-like behavior, rarely both. Critical State Soil Mechanics models such as Modified Cam Clay excel at capturing the quasi-static, history-dependent behavior of densely packed granular materials like soils, while rheological models such as the  $\mu(I)$  rheology capture dense granular flows. This study compares these two constitutive models via two numerical tests of increasing complexity: (1) homogeneous constant-pressure shear flow with varying inertial numbers and (2) a column collapse where spatial gradients evolve during time. We demonstrate that the  $\mu(I)$ -rheology with corrections describes the steady state and exhibits a large viscosity at low  $I$ . For such a model, the column collapse profile is smooth with diffuse shear bands. In contrast, Modified Cam Clay captures the consolidation history of the material. The collapse profile for the normally consolidated state shows layering and results in a bell-shaped pile, while the profile for the overconsolidated state shows chunk-like structures in the pile.

## 1 Introduction

Powders and grains are fascinating materials that exhibit solid-like and fluid-like behavior [1, 2]. Continuum theories capture the complexity of these materials on limiting states and can have significant engineering implications for consumer goods, various industries [3], or civil engineering phenomena, like geohazards.

Critical State Soil Mechanics (CSSM) [3, 4] has been instrumental in our understanding of the slow stress-deformation response of soils. Soil mechanics models, such as Modified Cam Clay, are rooted in critical state theory and allow us to model the consolidation history of soils under quasi-static conditions. However, the capability of CSSM models is limited to applications involving low shear rates.

Advancements in granular rheology have been extremely useful in modeling dense and inertial steady-state granular flows. The inertial number  $I$  serves as an indicator of the transition between quasi-static (solid-like) and inertial (fluid-like) states. The development of the  $\mu(I)$ -rheology has, from its earliest stages, seen attempts at including soil mechanics concepts [2, 5]; however, despite the progress, our conceptual understanding of how to relate and merge quasi-static and inertial models remains blurred.

In this paper, we study two well-known models, namely, the  $\mu(I)$ -rheology and the Modified Cam Clay model. They have the following fundamental differences:

- **Inertial and compressibility effects.** The  $\mu(I)$ -rheology relies on a sufficiently large  $I$  and sufficiently hard grains such that compressibility does not affect the

rheology [2, 6]. On the contrary, Modified Cam Clay refers to a regime where  $I$  is small and inertial effects are negligible during loading.

- **Transient and steady states.** The  $\mu(I)$  rheology operates in a steady state (dynamic equilibrium). In contrast, Modified Cam Clay begins at the static equilibrium and transitions through the elastic and elasto-plastic states to reach the quasi-static critical state.

Long-term goal is a unified model able to predict the material behavior across inertial regimes and deformation stages [7]. This study presents the two models and aims to highlight their potential strengths and weaknesses. We employ a constant pressure shear element test and a non-homogeneous granular collapse boundary value problem using the Material Point Method (MPM).

## 2 Models

### 2.1 Common notation

This work adopts the notation of Ref. [8], with a few exceptions. We follow the sign convention of soil mechanics with positive compressive stresses and strains. Furthermore, the tensor contraction is  $\cdot$ , the identity tensor is denoted as  $\mathbf{1}$ . The time derivative is  $\dot{\square} = \frac{\partial}{\partial t} \square$ , and we denote the increment as  $d\square$ . The Cauchy stress tensor  $\boldsymbol{\sigma}$  relates to the scalar pressure  $p = -\frac{1}{3}\text{trace}(\boldsymbol{\sigma})$ , and the deviatoric stress tensor  $\boldsymbol{s} = \boldsymbol{\sigma} + p\mathbf{1}$ . The deviatoric stress invariant is  $q = \sqrt{\frac{3}{2}\boldsymbol{s} : \boldsymbol{s}}$ . The strain tensor is  $\boldsymbol{\varepsilon}$ , and decomposes into a volumetric part  $\varepsilon_v = -\text{trace}(\boldsymbol{\varepsilon})$  and a deviatoric part  $\boldsymbol{\varepsilon}_d = \boldsymbol{\varepsilon} + \frac{1}{3}\varepsilon_v\mathbf{1}$ . The shear strain invariant is  $\gamma = \sqrt{\frac{1}{2}\boldsymbol{\varepsilon}_d : \boldsymbol{\varepsilon}_d}$ . We also denote elastic strains with  $(\cdot)^e$  and plastic strains with  $(\cdot)^p$ . Common rate terms are the shear strain tensor  $\dot{\boldsymbol{\varepsilon}}_d$  and the shear strain rate  $\dot{\gamma}$ .

\*e-mail: r.lubbe@utwente.nl

## 2.2 $\mu(I)$ - rheology

The  $\mu(I)$ -rheology has seen widespread adoption in the last decade [1, 2, 5, 9]. Central to this rheology is the dimensionless inertial number:

$$I(\dot{\gamma}, p) = \dot{\gamma} d_p / \sqrt{p/\rho_p}, \quad (1)$$

where  $d_p, \rho_p$ , are the particle diameter and density, respectively.

The " $\mu(I)$ " was born to describe steady, shear flows of hard collisional spheres [1, 2], leading to a relation between bulk friction and inertial number:

$$\mu(I) = \mu_0 + \frac{\mu_d - \mu_0}{\frac{I_0}{I} + 1}, \quad (2)$$

where  $I_0$  is the critical inertial constant, defining the transition from the quasi-static limit  $\mu(I \rightarrow 0) \sim \mu_0$ , to the inertial limit  $\mu(I \rightarrow \infty) \sim \mu_d$ .

Jop et al. [5] extended the  $\mu(I)$  rheology to a 3D tensorial form, employing a fluid-like constitutive relation:

$$\boldsymbol{\sigma} = -p\mathbf{1} + \eta \dot{\boldsymbol{\epsilon}}_d, \quad (3)$$

$$\eta(I, p) = \frac{\mu(I)p}{\dot{\gamma}}, \quad \mu(I) = \frac{1}{\sqrt{3}} \frac{q}{p} > \mu_0. \quad (4)$$

The above incorporates  $\mu(I)$  within the viscosity  $\eta(I, p)$  through two key assumptions: a Coulomb-type yield criterion is assumed, and the model assumes alignment of the tensor  $s$  and  $\dot{\boldsymbol{\epsilon}}_d$ .

A significant drawback of this model is that when  $I \rightarrow 0$  the viscosity  $\eta$  diverges. Franci et al. [9] proposed a regularization form for  $\mu$  that we will adopt in this work:

$$\eta(\dot{\gamma}, p) = \frac{\mu_0 p}{\sqrt{\dot{\gamma}^2 + \alpha^2}} + \frac{p(\mu_d - \mu_0)}{I_0 \sqrt{p/\rho_p + d_p \dot{\gamma}}}, \quad (5)$$

where  $\alpha = 0.0001 \text{ s}^{-1}$  is a (recommended) regularization parameter. Notice that  $\alpha = 0$  recovers the original form in Eq. (4). The proposed regularization addressed ill-conditioning while preserving solution accuracy in granular flow simulations [9].

A second limitation of the  $\mu(I)$ -rheology is that the model does not account for the material's compressibility. A simple solution is to use a linear compression (LC) law [10] to relate pressure  $p$  and solid volume fraction  $\phi$ :

$$p = K_{LC} \varepsilon_v = K_{LC} \left( \frac{\phi}{\phi_{\text{ref}}} - 1 \right), \quad (6)$$

where  $K_{LC}$  is the bulk modulus and  $\phi_{\text{ref}}$  is a reference solid volume fraction. The compressibility correction was validated in Ref. [10] through granular flow simulations. Ref. [6] supports a similar correction, which is validated through observation from discrete particle simulations.

## 2.3 Modified cam-clay

Modified Cam-Clay (MCC) is a well-known elastoplastic CSSM model for clays [4]. The elastoplastic transition is

defined by a yield surface, which is an ellipse in the  $q$ - $p$  space

$$F \equiv \frac{q^2}{M^2} - p(p_c - p) = 0, \quad (7)$$

and by the critical state (failure) line  $q/p = M = \sqrt{3}\mu_0$ . The slope of the critical state line  $M$  and pre-consolidation pressure  $p_c$  control the yield surface shape and size, respectively; as  $p_c$  changes, the yield surface expands (hardening) or contracts (softening).

An associated flow is assumed, where the yield surface coincides with the plastic potential

$$d\boldsymbol{\varepsilon}^p = \frac{\partial F}{\partial \boldsymbol{\sigma}} = d\Lambda \left[ \frac{3}{M^2} s + (2p - p_c) \mathbf{1} \right]. \quad (8)$$

where  $d\Lambda > 0$  is the plastic multiplier.

The model is built upon stress-history-dependent consolidation in the double natural logarithm specific volume  $v$  and pressure space  $\ln v - \ln p$  [4], defining normally consolidated initial states on the isotropic compression line (ICL, slope  $\lambda$ ) and overconsolidated states on the swelling line (OCL, slope  $\kappa$ ). The ratio ( $\text{OCR} = \frac{p_c}{p}$ ) quantifies overconsolidation. When sheared, along any stress path, the material fails on the critical state line CSL defined in the space  $\ln v - \ln p - q$ . The hardening and elastic pressure laws may be expressed as

$$dp_c = (\lambda - \kappa)^{-1} p_c d\varepsilon_v^p \quad \text{and} \quad dp = \kappa^{-1} p d\varepsilon_v^e, \quad (9)$$

Before yielding, a non-linear isotropic elastic behavior is assumed:

$$\boldsymbol{\sigma} = -K(p)\varepsilon_v^e \mathbf{1} + 2G(p)\boldsymbol{\varepsilon}_d^e, \quad (10)$$

where  $K(p)$  and  $G(p)$  are pressure-dependent bulk and shear moduli defined as  $K(p) = \frac{dp}{d\varepsilon_v^e} = \frac{p}{\kappa}$ , and  $G(p) = \frac{3(1-2\nu)}{2(1+\nu)} K(p)$ , where  $\nu$  is the Poisson's ratio.

## 3 Model parameters for a hypothetical granular material

The numerical tests were performed using the regularized  $\mu(I)$  rheology with the linear compression law denoted  $\mu(I)$ -LC, and MCC for materials with  $\text{OCR}=1$  and  $\text{OCR}=4$ . Table 1 shows the model parameters representing a hypothetical material, which we assume has  $\rho_p = 2450 \text{ kg/m}^3$ ,  $d_p = 0.005 \text{ m}$ . Model parameters were chosen to match in the regime where both models exhibit comparable pressure and density conditions.

Table 1: Model parameters for the hypothetical material:  $M = \sqrt{3}\mu_0$ ,  $M_d = \sqrt{3}\mu_d$ .

Model	$M$	$M_d$	$I_0$	$K_{LC}$ [kPa]	$\phi_{\text{ref}}$	$\lambda$	$\kappa$	$\nu$
$\mu(I)$ -LC	1.20	2.16	0.279	392	1.317	-	-	-
MCC	1.20	-	-	-	-	0.040	0.008	0.2

### 3.1 Constant pressure shear

We perform the element test at a constant pressure  $p = 1000 \text{ Pa}$ , and shear for total time  $t = 6.0 \text{ s}$  with a timestep

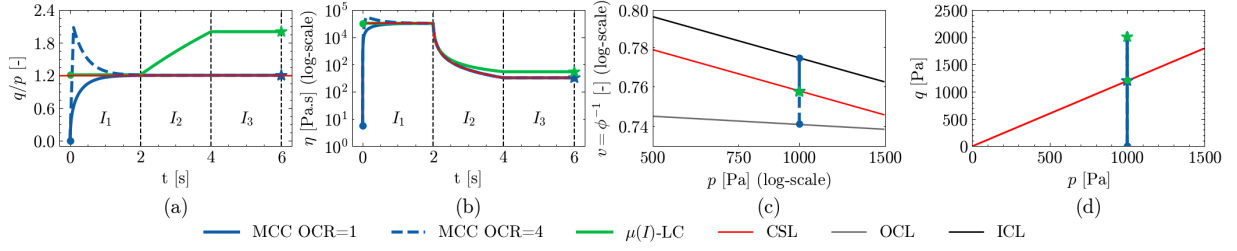


Figure 1: Constant pressure shear element test of  $\mu(I)$ -LC and MCC (OCR=1 and 4), over varying  $I(\dot{\gamma})$  stages. Initial states are marked with  $\bullet$ , and final states by  $\star$ . Lines connecting these markers show the evolution of variables during shearing. Projected CSL depicted in:  $q$ - $p$  vs.  $t$  (constant  $M$ ),  $\eta$  vs.  $t$  ( $p$  constant),  $\ln v$  vs.  $\ln p$  (slope  $\lambda$ ), and  $q$  vs.  $p$  (slope  $M$ ). The OCL (slope  $\kappa$ ) and ICL (parallel to CSL) are shown in  $\ln v$  vs.  $\ln p$ .

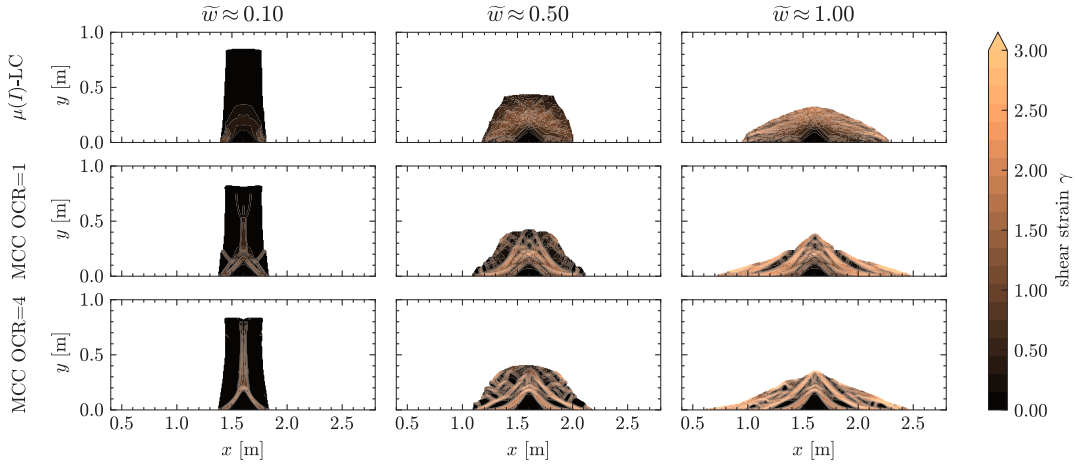


Figure 2: Snapshots of shear strain  $\gamma$  of the granular column collapse for  $\mu(I)$ -LC and MCC (OCR=1 and 4) at different normalized runout distances  $\tilde{w}$ , defined in Eq. (11).

$dt = 1 \times 10^{-5}$  s, while  $I$  is varied in stages: (1) initially constant  $I_1 = 0.001$  for 2.0 s; (2) linear ramp up to  $I_2 : 0.001 \rightarrow 0.1$  for 2.0 s; and (3) constant  $I_3 = 0.1$  for 2.0 s.

Fig. 1 (a) shows the ratio  $q/p$  vs time  $t$ , for the  $\mu(I)$ -LC model and MCC with OCR=1 and 4. In stage (1), MCC starts at  $q/p = 0$ , while  $\mu(I)$ -LC begins at  $q/p \neq 0$ .  $\mu(I)$ -LC remains unchanged for constant  $I$ . In contrast, MCC OCR=1 gradually increases until the critical state is reached, while OCR=4 overshoots elastically, then peaks and softens towards the critical state value  $M$ . Both OCR=1 and 4 converge to the critical state. In stages (2) and (3),  $\mu(I)$ -LC increases non-linearly with changing  $I$ , while MCC remains unchanged.

Fig. 1 (b) shows the viscosity  $\eta = \frac{1}{\sqrt{3}} \frac{q}{\dot{\gamma}}$  vs. time  $t$ . In stage (1),  $\mu(I)$ -LC begins at a constant  $\eta$  and stays unchanged with time. In contrast, MCC starts at small  $\eta$ ; OCR=1 and 4 follow a similar trend with a peak for OCR 4, and converge to a constant  $\eta$ . In stage (2), due to an inverse proportionality,  $\eta \propto \dot{\gamma}^{-1}$  decreases with increasing  $I \propto \dot{\gamma}$  in both models.  $\mu(I)$ -LC decreases much slower than MCC. In stage (3),  $\eta$  is constant, with  $\mu(I)$ -LC larger than MCC.

Fig. 1 (c) shows  $\ln v$  vs.  $\ln p$ . Overall,  $\mu(I)$ -LC remains constant. In contrast, the specific volume  $v$  reduces (contraction) to the CSL for the MCC OCR=1, while for OCR=4 starts on the OCL and dilates towards the CSL.

In  $q$  vs.  $p$  plot in Fig. 1 (d),  $\mu(I)$ -LC starts near the CSL and increase in  $q$ . In contrast, MCC OCR=1 and 4 start from the ICL and OCL at  $q = 0$  and converge at the CSL. Specifically, MCC OCR=1 approaches the CSL monotonously, while MCC OCR=4 overshoots and relaxes onto it.

Both models have different flow mechanisms. The  $\mu(I)$ -LC starts and develops from the critical state, and transitions between regimes with a change in  $I$ . In contrast, MCC exhibits small  $\eta$ , and the transient paths are distinct for different OCR but insensitive to  $I$ .

### 3.2 Granular collapse

We simulate a simple boundary value problem, namely granular collapse, using the Material Point Method (MPM) with the publicly available code, *HydraxMPM* [7]. Simulations assume plane strain, and a column 0.3 m (width)  $\times$  0.9 m (height). We use a cell size of 0.00625 m and four material points per cell as the initial configuration. We apply a friction coefficient of 0.7 to the floor to simulate a non-smooth base. The material points' initial vertical stress is obtained by  $\sigma_{yy}^0 = \rho_g g (h_{mp} - z)$ , with their height  $h_{mp}$ , column height  $z$ , column bulk density  $\rho_g = 1500 \text{ kg/m}^3$ , and gravity  $g = 9.8 \text{ m/s}^2$ .  $\sigma_{xx}^0 = \sigma_{yy}^0$  gives the initial horizontal normal stress. For MCC, the initial out-of-plane stress is  $\sigma_{zz}^0 = \nu(\sigma_{xx}^0 + \sigma_{yy}^0)$ , while  $\mu(I)$ -LC  $\sigma_{zz}^0 = \sigma_{yy}^0$ . The difference in  $\sigma_{zz}^0$  stems from the

MCC's reliance on elasticity theory to enforce plane strain ( $\varepsilon_{zz} = 0$ ), a constraint not explicitly required by  $\mu(I)$ -LC. We interpolate the material point positions and deformation gradients to the grid to find the shear strain  $\gamma$ , and calculate the normalized horizontal spread as

$$\bar{w} = \frac{w(t) - w_0}{w_{\max} - w_0}, \quad (11)$$

where  $w_0$ ,  $w_{\max}$ ,  $w(t)$  are the initial, final and time-varying spreads of the column. A column is at its minimum spread at  $\bar{w} = 0$ , while it is at its maximum spread  $\bar{w} = 1$ . Fig. 2 shows snapshots of the column collapse simulations.

**$\mu(I)$ -LC:** At  $\bar{w} \approx 0.1$ , weak shear banding is visible. At  $\bar{w} \approx 0.5$ , the bulk of the column exhibits a dense network of shear bands. Last, at  $\bar{w} \approx 1.0$ , the shape has a smooth convex geometry with a rounded tip.

**MCC OCR=1:** At  $\bar{w} \approx 0.1$ , the column exhibits triangular shear bands at the base. At  $\bar{w} \approx 0.5$ , retrogressive layers emerge, a phenomenon where the failure surface progresses in a step-wise manner. Finally, at  $\bar{w} \approx 1.0$ , a concave pile forms with curved shear bands extending outward and sideways.

**MCC OCR=4:** At  $\bar{w} \approx 0.1$ , the column exhibits significant fracturing and triangular shear bands near its base. At  $\bar{w} \approx 0.5$ , the collapse progresses with chunks. Then, at  $\bar{w} \approx 1.0$ , the final pile forms with chunk structures still visible.

The  $\mu(I)$ -LC column collapse exhibits a smooth profile. In contrast, MCC OCR=1 and 4 display distinct interesting responses. The normally consolidated state (OCR=1) flows more steadily, resulting in a confined shape, and its shear strain values are more distributed. Its pile has high-intensity shear patterns and a central depression. On the contrary, the overconsolidated state (OCR=4) forms chunks.

## 4 Conclusion and outlook

This paper numerically investigates two well-known constitutive models for granular materials, namely, the  $\mu(I)$  rheology and Modified Cam Clay (MCC). We compare their strengths and weaknesses through constant pressure element tests and granular column collapse simulations using the Material Point Method. The motivation for this paper is to compare the limit behaviors of the models, beyond their conventional application regimes/states with the final goal of a unified model.

The  $\mu(I)$ -rheology operates in steady state and would require multiple corrections to model a compressible material in quasi-static conditions. The element test shows that the corrected model including  $p(\phi)$  and regularized viscosity  $\eta$  has a constant  $\eta$  near the static limit and a lower  $\eta$  when  $I$  increases. The column collapse profile was smooth with distributed weak shear bands.

In contrast, the MCC operates in the static, transient, and critical (steady) state at small shear rates. Depending on the overconsolidation ratio, hardening or softening is observed, resulting in distinct transient viscosities during shear. The column collapse profile of the normally consolidated sample exhibits layering of shear bands, as well as intense, distributed shear bands with a central depression.

In contrast, the overconsolidated sample shows chunks in the pile.

A limitation of this study is the use of hypothetical material. Application to realistic materials, including calibration, will be part of future work [11]. The primary focus of this work is not prediction but rather understanding and comparing via element test how these models behave in a boundary value problem, even when operating outside their conventional pressure and density ranges.

Our future direction involves a unified model [11], that will be rooted on two key elements: (1) combining transient and steady states, at the level of a yield surface and  $I$ -dependent steady state; (2) merging inertial and compressibility effects, via a shared pressure-dilatancy law.

## Acknowledgements

This research is part of the project TUSAIL (Training in Upscaling Particle Systems: Advancing Industry across Length-scales) and has received funding from the European Horizon2020 Framework Programme under grant agreement ID 955661.

## References

- [1] GDR MiDi, On dense granular flows, *The European Physical Journal E* **14**, 341 (2004). [10.1140/epje/i2003-10153-0](https://doi.org/10.1140/epje/i2003-10153-0)
- [2] F. Da Cruz, S. Emam, M. Prochnow, J.N. Roux, F. Chevoir, Rheophysics of dense granular materials: Discrete simulation of plane shear flows, *Physical Review E* **72**, 021309 (2005).
- [3] A.N. Schofield, P. Wroth, *Critical state soil mechanics*, Vol. 310 (McGraw-Hill London, 1968)
- [4] G.T. Houlsby, A.M. Puzrin, *Advanced Plasticity Theories* (Springer, 2007)
- [5] P. Jop, Y. Forterre, O. Pouliquen, A constitutive law for dense granular flows, *Nature* **441**, 727 (2006). [10.1038/nature04801](https://doi.org/10.1038/nature04801)
- [6] H. Shi, S. Roy, T. Weinhart, V. Magnanimo, S. Luding, Steady state rheology of homogeneous and inhomogeneous cohesive granular materials, *Granular Matter* **22**, 1 (2020).
- [7] R. Lubbe, H. Cheng, Grainlearning/hydraxmpm: Hydraxmpm v0.2.0-alpha (2025), <https://doi.org/10.5281/zenodo.15207774>
- [8] E.A. de Souza Neto, D. Peric, D.R. Owen, *Computational methods for plasticity: theory and applications* (John Wiley & Sons, 2011)
- [9] A. Franci, M. Cremonesi, 3D regularized  $\mu(I)$ -rheology for granular flows simulation, *Journal of Computational Physics* **378**, 257 (2019).
- [10] A.M. Salehizadeh, A.R. Shafiei, Modeling of granular column collapses with  $\mu(I)$  rheology using smoothed particle hydrodynamic method, *Granular Matter* **21**, 32 (2019). [10.1007/s10035-019-0886-6](https://doi.org/10.1007/s10035-019-0886-6)
- [11] R. Lubbe, H. Cheng, S. Luding, V. Magnanimo, A pressure-shear-dilation rate-dependent model for transient granular solid-fluid behavior (2025), in preparation